Supporting information for:

# Exploration of an Easily Synthesized Fluorescent Probe for Detecting Copper in Aqueous Samples

Jesus Sanmartín-Matalobos.* Ana M. García-Deibe. Matilde Fondo. Morteza Zarepour-Jevinani

M. Raquel Domínguez-González and Pilar Bermejo-Barrera

*jesus.sanmartin@usc.es

**Table S1**.  Main bond distances [Å] and angles [°] for $Pd_2(L)_2$

| Atoms | Distance | Atoms | Distance |
|---|---|---|---|
| Pd1-N13 | 2.009(3) | Pd2-N23 | 1.993(3) |
| Pd1-N12 | 2.023(3) | Pd2-N22 | 2.036(3) |
| Pd1-N21 | 2.074(3) | Pd2-N21 | 2.074(3) |
| Pd1-N11 | 2.080(3) | Pd2-N11 | 2.114(3) |
| Pd1···Pd2 | 3.0000(8) | | |
| N11-S11 | 1.681(3) | N21-S21 | 1.681(3) |
| N11-C107 | 1.509(4) | N21-C207 | 1.505(4) |
| C101-S11 | 1.778(3) | C201-S21 | 1.767(3) |
| C113-N12 | 1.421(4) | C213-N22 | 1.424(4) |
| N12-C114 | 1.320(4) | N22-C214 | 1.309(4) |
| N13-C115 | 1.387(4) | N23-C215 | 1.384(4) |
| N13-C118 | 1.342(4) | N23-C218 | 1.338(4) |
| Atoms | Angle | Atoms | Angle |
| N13-Pd1-N12 | 81.27(11) | N23-Pd2-N22 | 80.63(11) |
| N13-Pd1-N21 | 97.92(10) | N23-Pd2-N21 | 174.54(11) |
| N12-Pd1-N21 | 169.24(10) | N22-Pd2-N21 | 93.92(11) |
| N13-Pd1-N11 | 173.42(11) | N23-Pd2-N11 | 100.32(10) |
| N12-Pd1-N11 | 94.04(10) | N22-Pd2-N11 | 168.08(10) |
| N21-Pd1-N11 | 85.06(10) | N21-Pd2-N11 | 84.97(10) |
| Pd1-N11-Pd2 | 91.32(10) | Pd1-N21-Pd2 | 92.67(10) |

**Table S2**.  Main bond distances [Å] and angles [°] for Co(L)(HL)(H$_2$O)

| Atoms | Distance | Atoms | Angle |
|---|---|---|---|
| Co1-N14 | 1.90(3) | Co2-N21 | 1.91(3) |
| Co1-N11 | 1.93(2) | Co2-N24 | 1.92(3) |
| Co1-N12 | 1.97(3) | Co2-O2W | 1.96(2) |
| Co1-N13 | 1.98(3) | Co2-N25 | 1.98(2) |
| Co1-O1w | 1.98(2) | Co2-N23 | 2.00(3) |
| Co1-N15 | 1.99(2) | Co2-N22 | 2.01(2) |
| **Atoms** | **Angle** | **Atoms** | **Angle** |
| N11-Co1-N13 | 170.0(11) | N21-Co2-N23 | 170.0(11) |
| O1w-Co1-N15 | 171.5(10) | N24-Co2-N22 | 171.0(11) |
| N14-Co1-N12 | 174.2(11) | O2W -Co2-N25 | 171.9(10) |

**Table S3**. Diffraction data for $Pd_2L_2$ and $Co(L)(HL)(H_2O)$

|  | $Pd_2(L)_2$ | $Co(L)(HL)(H_2O)$ |
|---|---|---|
| Formula | $C_{38}H_{34}N_6O_4Pd_2S_2$ | $C_{38}H_{37}CoN_6O_5S_2$ |
| Molecular weight (g/mol) | 915.63 | 780.78 |
| Crystal system | Monoclinic | Monoclinic |
| Space group | $P2_1/n$ | $Pc$ |
| a (Å) | 12.8836(7) | 10.3758(9) |
| b (Å) | 15.6534(9) | 10.3171(8) |
| c (Å) | 17.2288(9) | 33.283(3) |
| α (°) | 90 | 90 |
| β (°) | 90.186(3) | 97.525(7) |
| γ (°) | 90 | 90 |
| Volume (Å³) | 3474.55(45) | 3532.2(5) |
| Z | 4 | 4 |
| Calc. Density (g/cm³) | 1.750 | 1.468 |
| Absorption Coeff. µ (mm⁻¹) | 1.208 | 0.658 |
| $F(000)$ | 1840 | 1624 |
| $2\theta_{max}/°$ | 52.82 | 50.56 |
| All refl. / Indepedent refl. | 51922 / 7096 | 13764 / 11883 |
| $R_{int}$ | 0.0320 | 0.0833 |
| Data / restraints / parameters | 7096 / 0 / 470 | 13764 / 2305 / 962 |
| Final R Indices $[I > 2\sigma(I)]$ | 0.0313. 0.0609 | 0.1245. 0.2683 |
| R Indices. all data | 0.0541. 0.0678 | 0.1565. 0.2951 |
| Máx. Residuals (e.Å⁻³) | 0.579. -0.586 | 1.807, -2.055 |
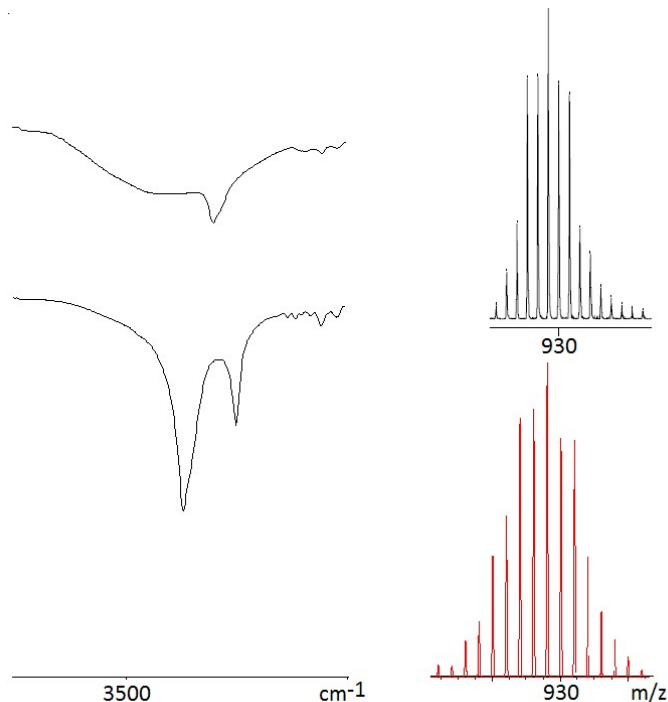
**Fig. S1.** *Left*: Partial view of the infrared spectra of $H_2L$ (bottom) and $Cu(HL)_2$ (top), showing the presence of $\nu(NH)_{sulfonamide}$ (at 3310 cm$^{-1}$) and the absence of $\nu(NH)_{pyrrole}$ in the complex. *Right*: Partial view of the mass spectrum of $Cd_2(L)_2 \cdot 4H_2O$ showing the found (top) and the calculated (bottom) molecular ion peak.

The good agreement between found and calculated isotopic profile of the peak attributed to $Cd_2(L)_2$ (Fig. S1, right), representing $M_2(L)_2$ complexes, is a clear sign of the obtaining of a dinuclear complex. Monodeprotonation of the ligand in $Cu(HL)_2$, representing $M(HL)_2$ complexes, is easy to see because pyrrole $\nu(NH)$ band is absent in its infrared spectrum (Fig. S1, left), while sulfonamide $\nu(NH)$ band is present at about 3310 cm$^{-1}$. Since sulfonamide $\nu(NH)$ band undergoes *ca.* 52 cm$^{-1}$ shift to higher frequencies, a hydrogen bond has been deduced.
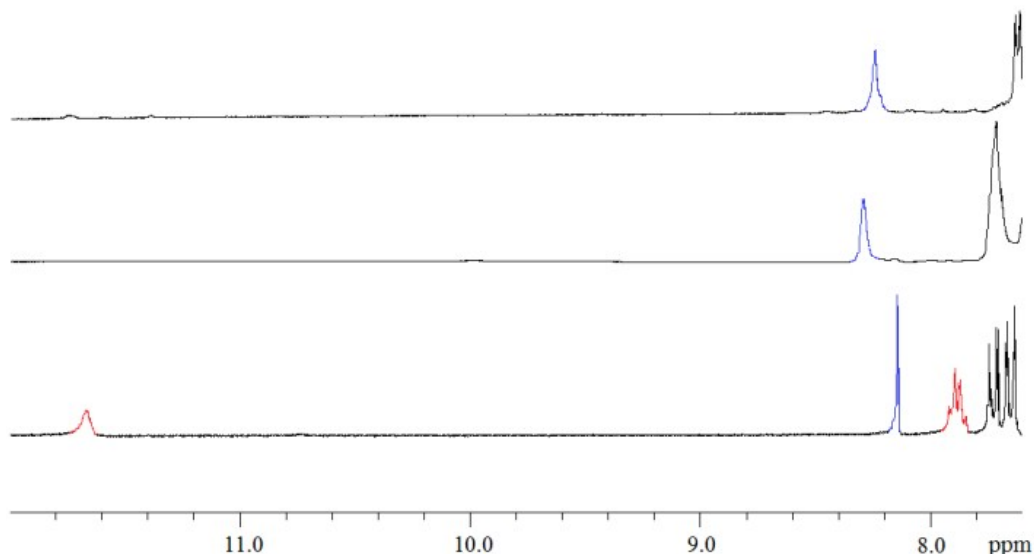
**Fig. S2**. Partial view of the $^1$H NMR spectra of $H_2L$ (bottom), $Co(L)(HL)(H_2O)$ (medium) and $Cd_2(L)_2 \cdot 4H_2O$ (top). Signals of $NH_{pyrrol}$ (11.68 ppm) and $NH_{sulfonamide}$ (7.88 ppm) are highlighted in red, while imino signals are highlighted in blue.

Fig. S2 shows the absence of $NH_{pyrrol}$ (11.68 ppm) and $NH_{sulfonamide}$ (7.88 ppm) signals in the spectrum of $Cd_2(L)_2 \cdot 4H_2O$. The azomethine -CH=N signal which observed at 8.15 ppm in $H_2L$ undergoes shift to the low field (about 0.1 ppm), thus, indicating coordination of the ligand through the imine nitrogen atom. It must be noted that in $Co(L)(HL)(H_2O)$ one of the ligand molecules is acting as a dianionic tridentate chelating ligand and the other one is acting as a monoanionic bidentate chelating ligand. Although the sulfonamide functional group $NH_{sulfonamide}$ remains protonated in the monoanionic form HL (as signals integration shown), an overlap with tosyl signal (H2+H6) prevents its observation in $Co(L)(HL)(H_2O)$.
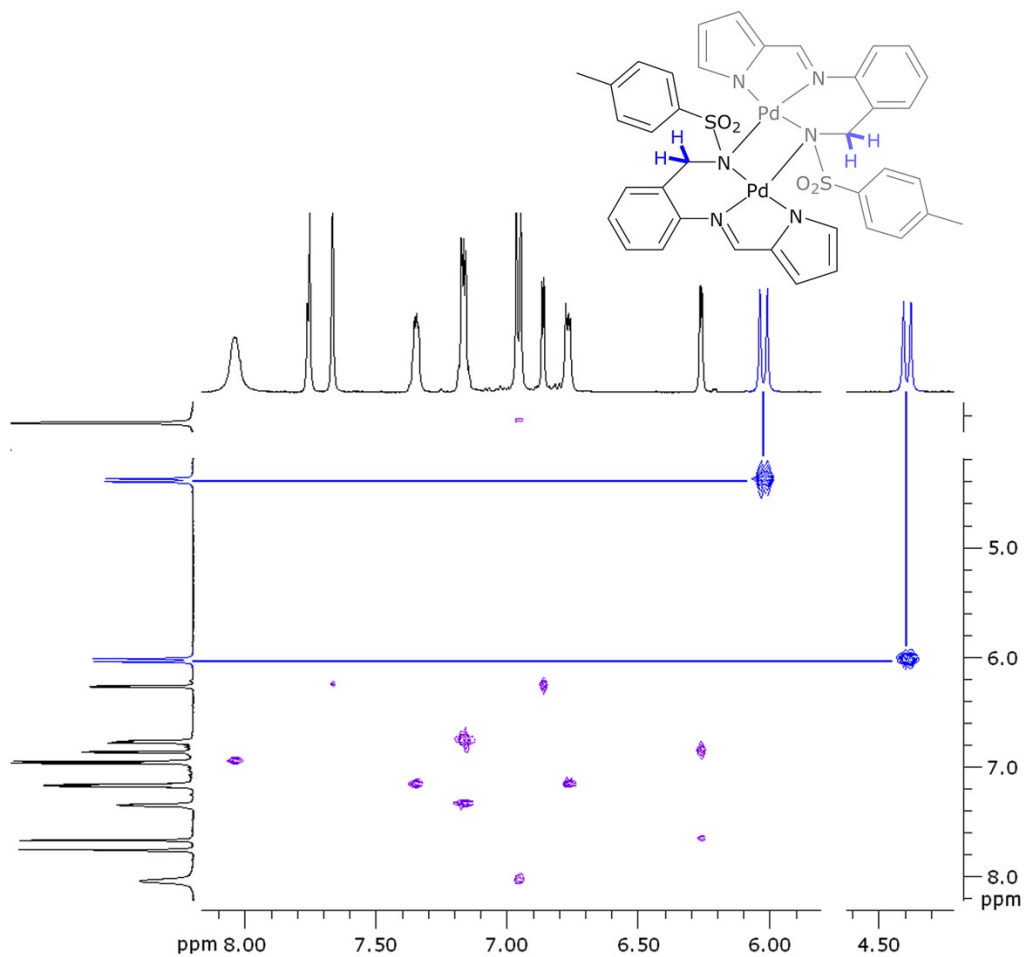
**Fig. S3.** Partial view of the COSY spectrum of Pd$_2$(L)$_2$.

The 2D COSY spectrum of Pd$_2$(L)$_2$ in dmso-d$_6$ at room temperature revealed two different chemical shifts for the two geminal protons of the methylenes (δ about 4.4 and 6.0 ppm; J about 14 Hz), despite being not placed in a chiral environment, and therefore are diastereotopic protons.
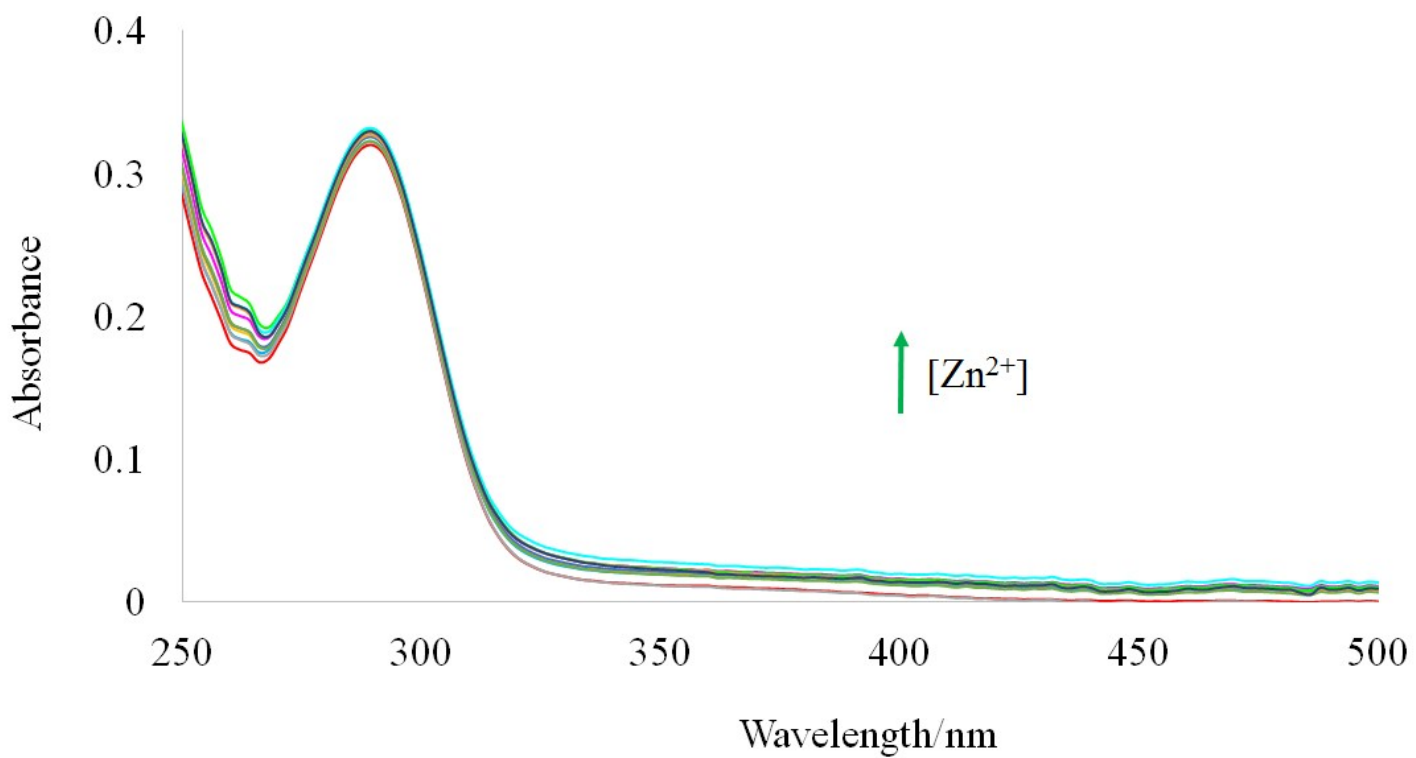
**Fig. S4.** Partial view of the absorption spectra of $H_2L$ (100 μM,) before and after addition of $Zn^{2+}$ (100 μM), measured in methanol (pH 7.0-7.5). Spectral data were recorded at 10 minutes after the addition of $Zn^{2+}$ (0.0, 0.1, 0.2, 0.3, 0.4, 0.5, 0.6, 0.7, 0.8, 0.9, 1.0, 1.5, 2.0 mL) to $H_2L$ (1.0 mL) at room temperature.
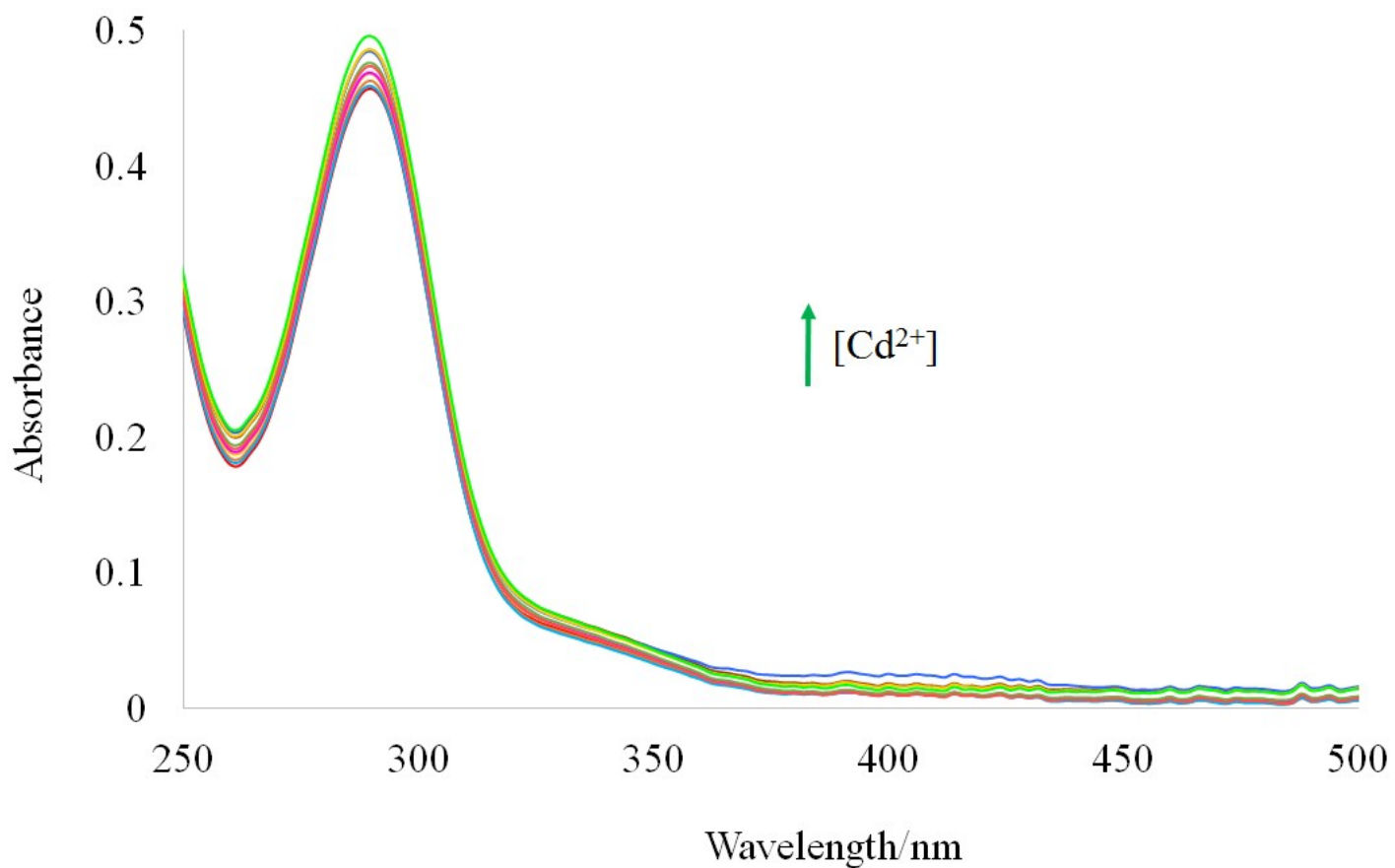
**Fig. S5.** Partial view of the absorption spectra of $H_2L$ (100 μM,) before and after addition of $Cd^{2+}$ (100 μM), measured in methanol (pH 7.0-7.5). Spectral data were recorded at 10 minutes after the addition of $Cd^{2+}$ (0.0, 0.1, 0.2, 0.3, 0.4, 0.5, 0.6, 0.7, 0.8, 0.9, 1.0, 1.5, 2.0 mL) to $H_2L$ (1.0 mL) at room temperature.
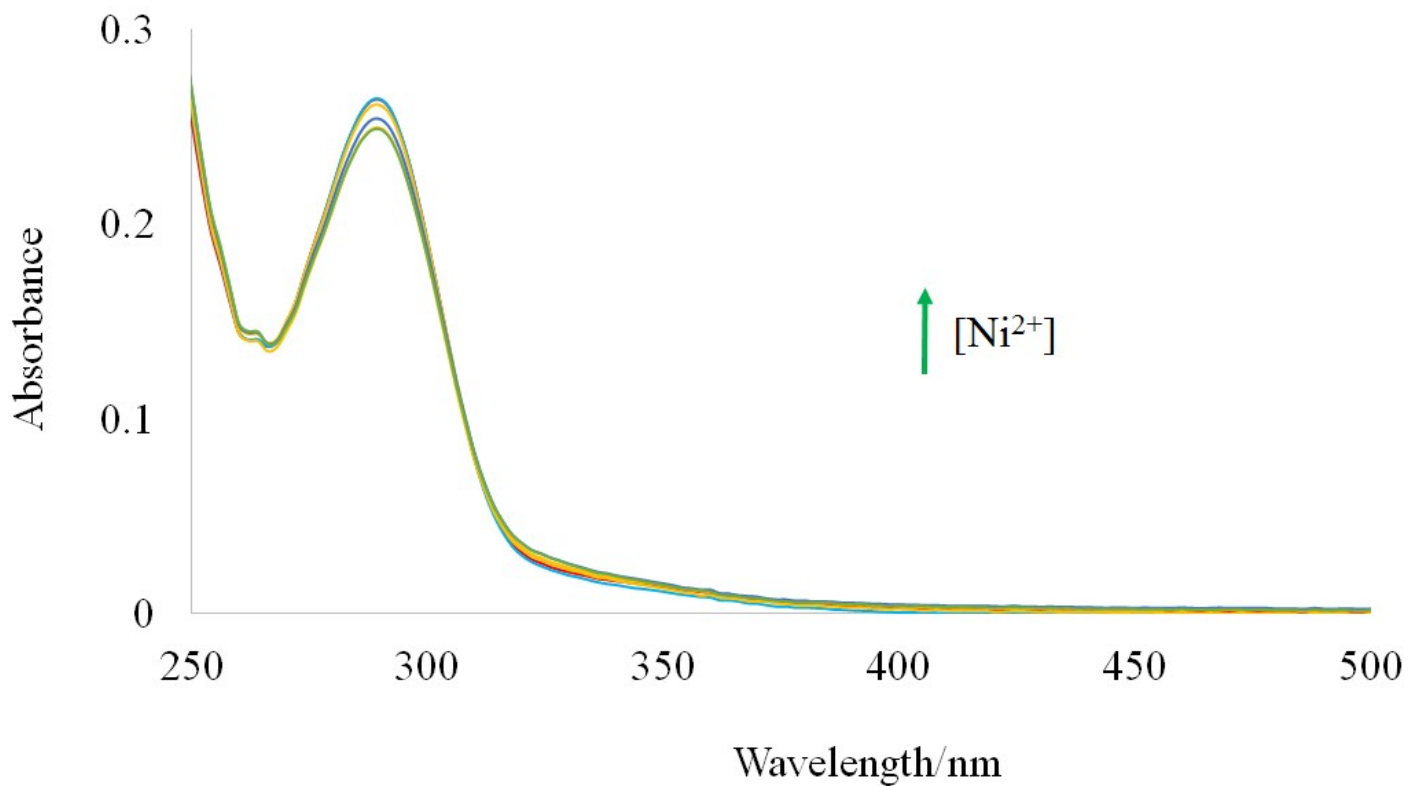
**Fig. S6**. Partial view of the absorption spectra of $H_2L$ (100 μM,) before and after addition of $Ni^{2+}$ (100 μM), measured in methanol (pH 7.0-7.5). Spectral data were recorded at 10 minutes after the addition of $Ni^{2+}$ (0.0, 0.1, 0.2, 0.3, 0.4, 0.5, 0.6, 0.7, 0.8, 0.9, 1.0, 1.5, 2.0 mL) to $H_2L$ (1.0 mL) at room temperature.
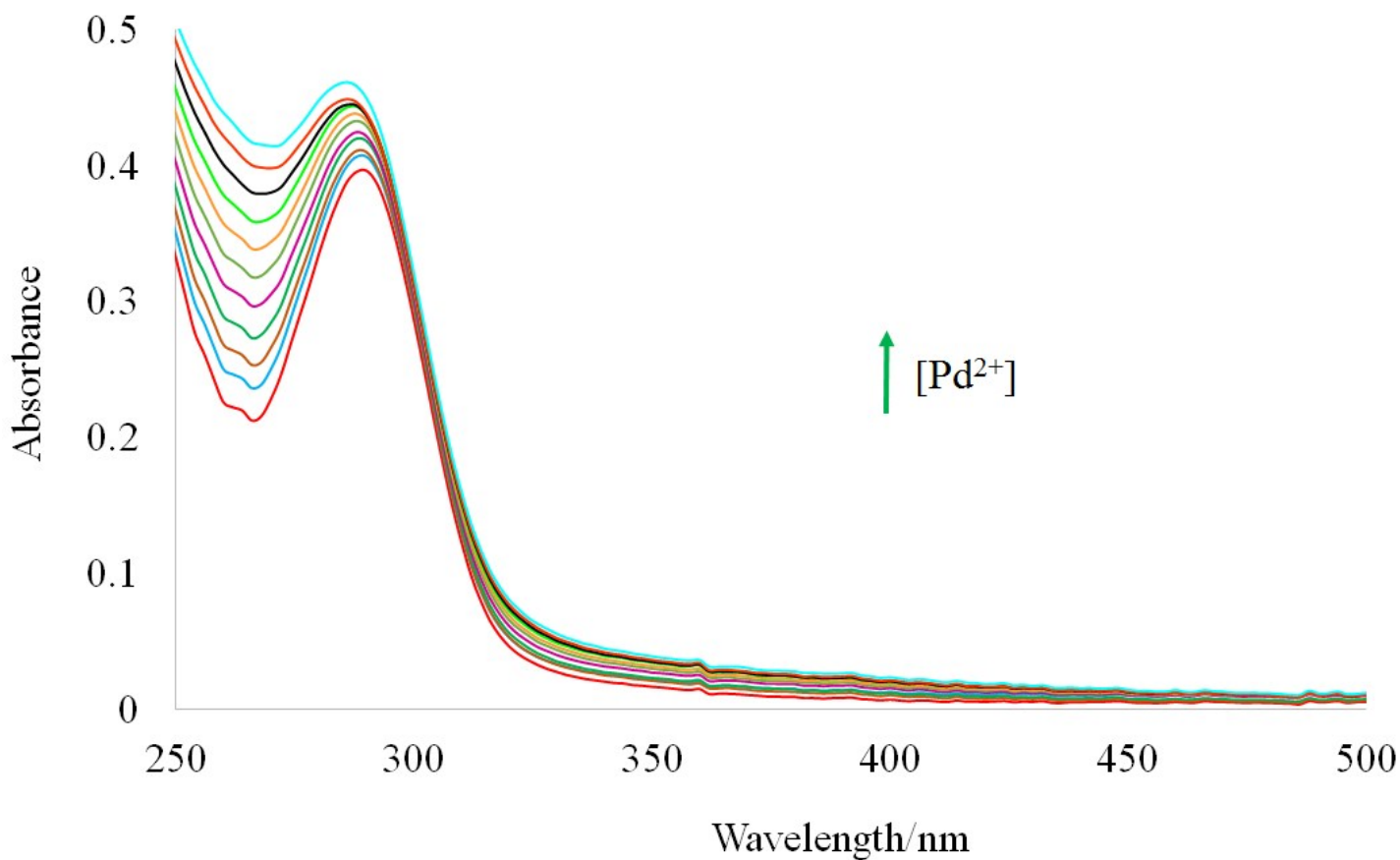
**Fig. S7**. Partial view of the absorption spectra of $H_2L$ (100 μM,) before and after addition of $Pd^{2+}$ (100 μM), measured in methanol (pH 7.0-7.5). Spectral data were recorded at 10 minutes seconds after the addition of $Pd^{2+}$ (0.0, 0.1, 0.2, 0.3, 0.4, 0.5, 0.6, 0.7, 0.8, 0.9, 1.0, 1.5, 2.0 mL) to $H_2L$ (1.0 mL) at room temperature.
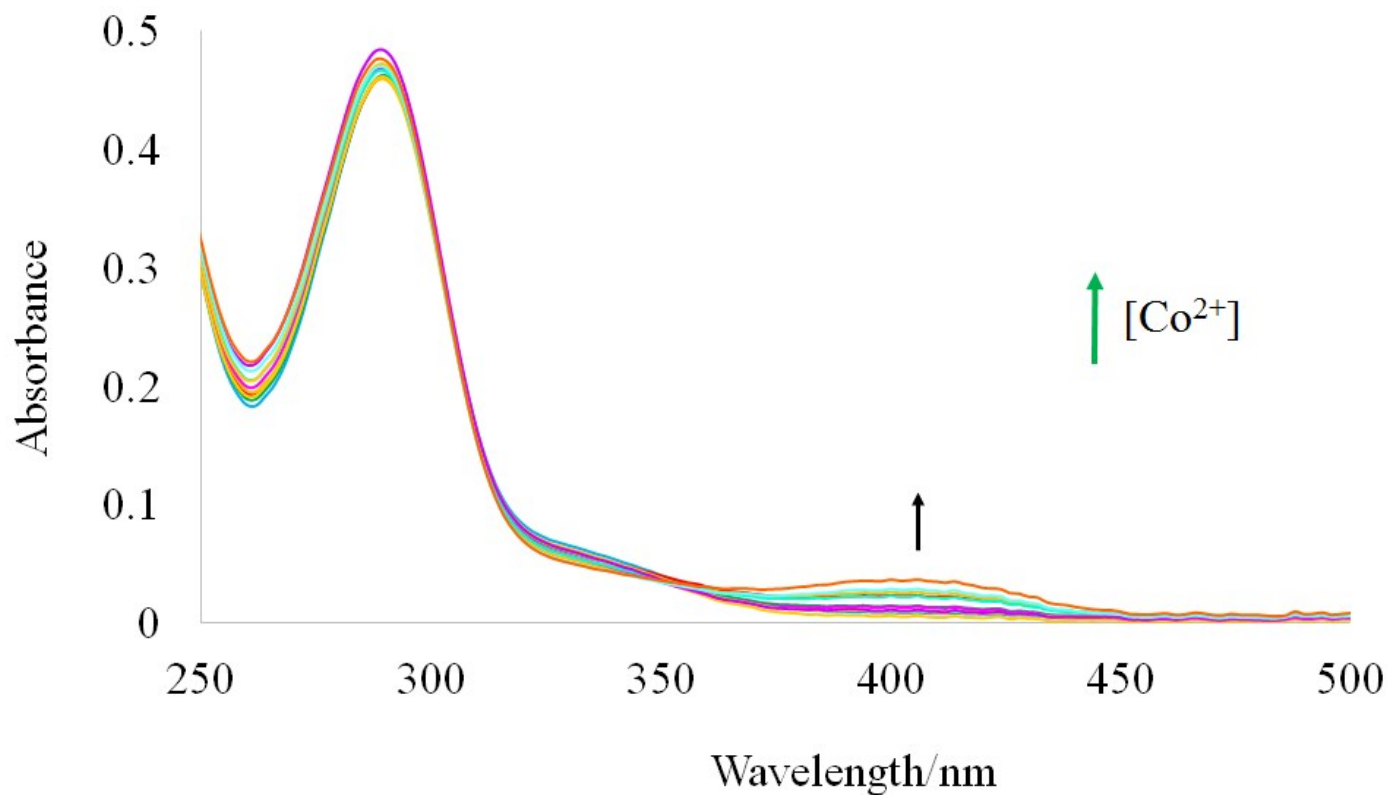
**Fig. S8**. Partial view of the absorption spectra of H$_2$L (100 μM,) before and after addition of Co$^{2+}$ (100 μM), measured in methanol (pH 7.0-7.5). Spectral data were recorded at 10 minutes after the addition of Co$^{2+}$ (0.0, 0.1, 0.2, 0.3, 0.4, 0.5, 0.6, 0.7, 0.8, 0.9, 1.0, 1.5, 2.0 mL) to H$_2$L (1.0 mL) at room temperature.
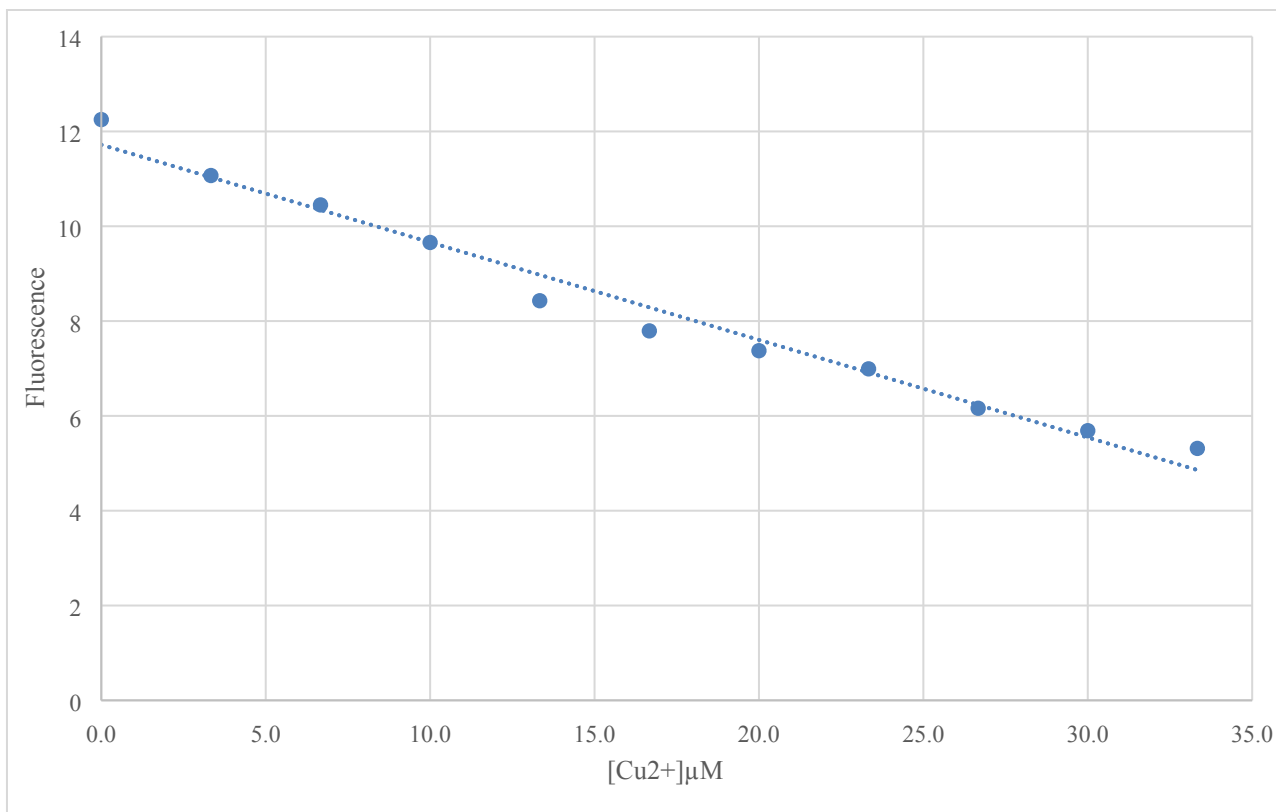
**Fig. S9**. Plot of emission intensity of $H_2L$ (100 µM) upon gradual addition of $Cu^{2+}$ (100 µM). Spectral data were recorded at about ten minutes after the addition of $Cu^{2+}$ (0.0, 0.1, 0.2, 0.3, 0.4, 0.5, 0.6, 0.7, 0.8, 0.9 and 1.0 mL) to $H_2L$ (1.0 mL). The limits of detection (LOD) and quantification (LOQ) were calculated according to LOD = 3SD/$m$ and LOQ = 10SD/m, where SD is the standard deviation of eleven measurements of a blank and m is the slope of the calibration graph.

LOQ(mg/l)=  1,84E-03  LOD(mg/l)  5,51E-04
LOQ(µM)=     2,89E-02  LOQ(µM)    8,67E-03
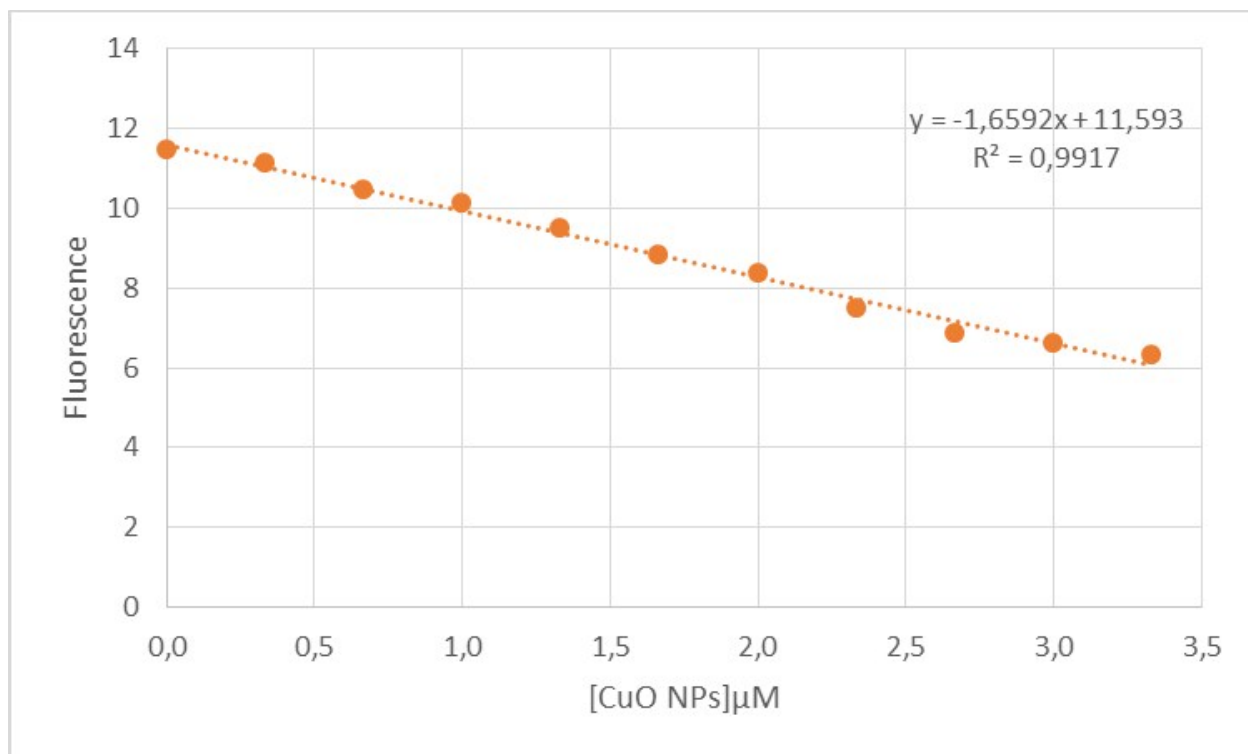
**Fig. S10**. Plot of emission intensity of $H_2L$ (100 µM) upon gradual addition of CuO NPs (100 µM). Spectral data were recorded at about ten minutes after the addition of $Cu^{2+}$ (0.0, 0.01, 0.02, 0.03, 0.04, 0.05, 0.06, 0.07, 0.08, 0.09 and 0.1 mL) to $H_2L$ (1.0 mL). The limits of detection (LOD) and quantification (LOQ) were calculated according to LOD = 3SD/$m$ and LOQ = 10SD/m, where SD is the standard deviation of eleven measurements of a blank and m is the slope of the calibration graph.

| | | | |
|---|---|---|---|
| LOQ CuO NPs (mg/l)= | 0.0461 | LOD CuONPs (mg/l) | 0.014 |
| LOQ CuO NPs (µM)= | 0.5798 | LOD CuONPs (µM/l) | 0.174 |
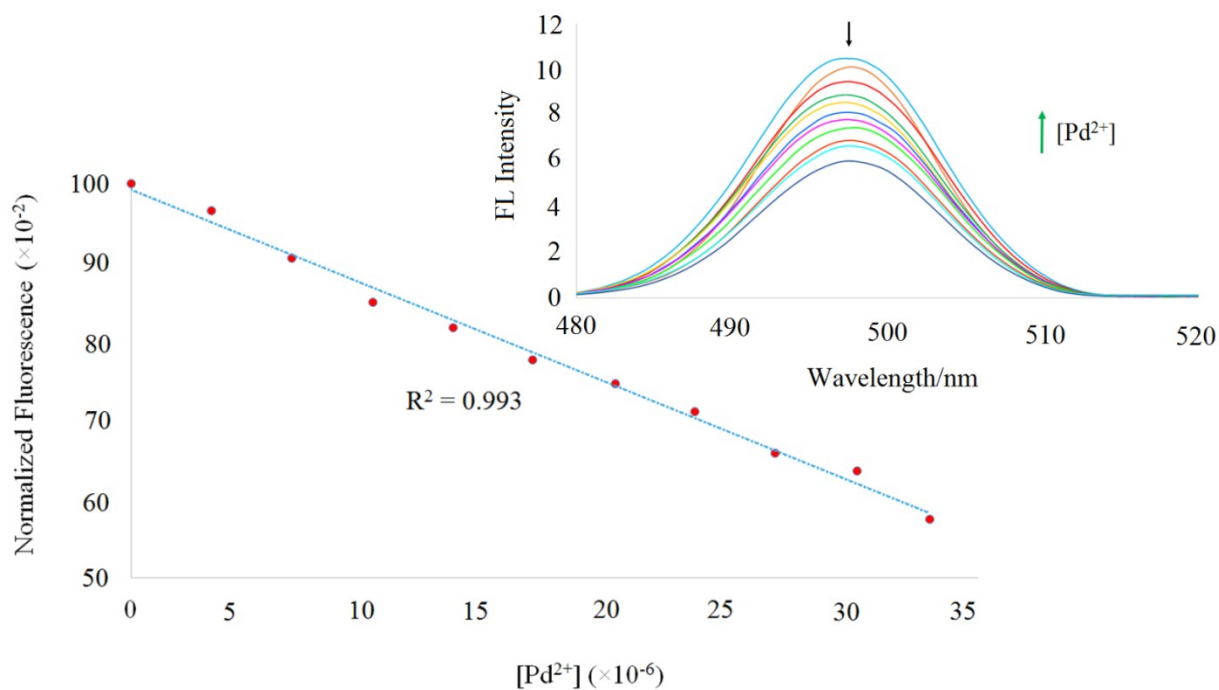
**Fig. S11**. The linear relationship between fluorescence intensity and $Pd^{2+}$ concentrations measured in methanol (pH 7.0-7.5) under $\lambda_{exc}$ = 378 nm. *Inset:* Fluorescence titration spectra of $H_2L$ (100 µM) with gradual addition of $Pd(OAc)_2$ (100 µM). Spectral data were recorded at 60 seconds after the addition of $Pd^{2+}$ (0.0, 0.1, 0.2, 0.3, 0.4, 0.5, 0.6, 0.7, 0.8, 0.9 and 1.0 mL) to $H_2L$ (1.0 mL) at room temperature.

The changes in the fluorescence spectrum of $H_2L$ upon titration with nickel(II) acetate tetrahydrate and cobalt(II) acetate tetrahydrate were similar to the observed after the addition of $Pd^{2+}$.
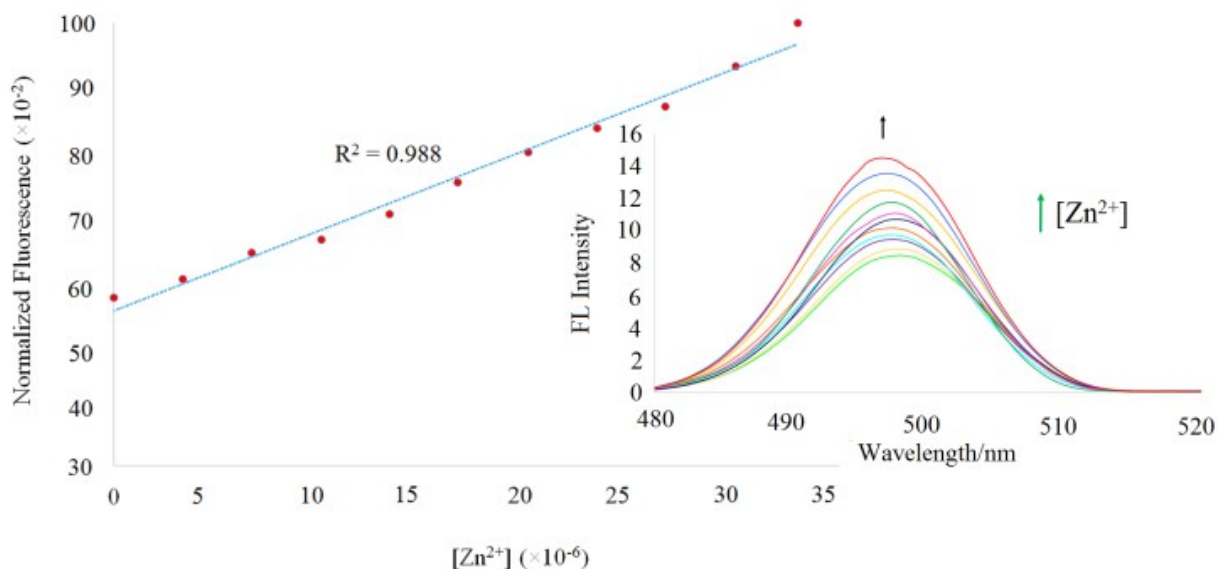
**Fig. S12**. The linear relationship between normalized fluorescence intensity and $Zn^{2+}$ concentrations measured in methanol (pH 7.0-7.5) under $\lambda_{exc} = 378$ nm. *Inset:* Fluorescence titration spectra of $H_2L$ (100 μM) with gradual addition of $Zn(OAc)_2 \cdot 2H_2O$ (100 μM). Spectral data were recorded at about ten minutes after the addition of $Zn^{2+}$ (0.0, 0.1, 0.2, 0.3, 0.4, 0.5, 0.6, 0.7, 0.8, 0.9 and 1.0 mL) to $H_2L$ (1.0 mL) at room temperature.

The changes in the fluorescence spectrum of $H_2L$ upon titration with $Zn^{2+}$ ions are shown in Fig. S11. It is apparent that with increasing $Zn^{2+}$ ion concentration, the fluorescence intensity of $H_2L$ at 498 nm increased. The fluorescence intensity varied linearly with the concentrations of $Zn^{2+}$ ions below 33 μM (2.1 mg/L), increasing by over 40%. The changes in the fluorescence spectrum of $H_2L$ upon titration with cadmiun(II) acetate dihydrate, were similar to the observed after the addition of $Zn^{2+}$. However, enhancement of the fluorescence was lower than the observed in the presence of $Zn^{2+}$, and therefore no further studies were performed on $H_2L$ upon titration with $Cd^{2+}$.